

Supplementary Materials

Supplementary Materials and Methods

Blood parameters

Mouse whole blood white blood cell count was measured using an automatic blood cell analyzer (KX-21, Japan).

Immunofluorescence of tissue sections

Femur and tibia tissues dissected from mice were fixed using 4% paraformaldehyde in PBS at 4°C for 24 h and decalcified in 15% EDTA (pH 7.4) at 4°C for 14 days. The tissues were embedded in paraffin and 5- μ m sagittal-oriented sections were prepared for histological analyses. For immunofluorescence, we incubated the samples with primary antibodies against the following proteins: Dmp1 (AF4386; R&D Systems), IL-19 (MA5-24093; Thermo Fisher Scientific, Waltham, MA, USA), P-S6 (AF3918; R&D Systems), Gr-1, and p-STAT3 (Y705) (AP0070; Abclonal, College Park, MD, USA), following by incubation by secondary antibodies for 1 h in the dark. After labeling, cells were incubated with DAPI for 5 min. The images were acquired with an Olympus 200 M microscope. The numbers of positively-stained cells in the whole medullary space or bone trabecula per femur or tibia were counted in three sequential sections per mouse in each group with Image Pro Plus software.

Hematoxylin and eosin (H&E) staining

Long bones were fixed with 4% paraformaldehyde for 24 h, decalcified with 0.5 M EDTA at pH 7.4 for 14 days, and embedded in paraffin. Five-micrometer-thick sections were cut for H&E staining. The number of osteocytes were averaged from five different areas per slide following microscopic evaluation at 400 \times magnification.

Quantitative RT-PCR

Total RNA was extracted from cells and tissues using the RNA-plus solution. Equal amounts of total RNA for each sample was used for oligo-d(T) primed reverse transcription into cDNA using SuperScript II (R123, Q341; Vazyme Biotech Co., Ltd., Nanjing, China). Primers for

real-time PCR were obtained from Integrated DNA Technologies. Reactions were run on an Applied Biosystems Prism machine using SYBR Green Master Mix (Applied Biosystems, Foster City, CA, USA). The amount of GAPDH cDNA was used to normalize results from gene-specific reactions. Primer sequences used to produce gene-specific amplicons are as follows: IL-19: forward, CTCCTGGGCATGACGTTGATT; reverse, GCATGGCTCTCTTG-ATCTCGT; GAPDH: forward, AAATGGTGAAGGTCGGTGTGAAC; reverse, CAACAAT-CTCCACTTTGCCACTG; Cathepsin K: forward, GGCCAACTCAAGAAGAAAAC; reverse, GTGCTTGCTTCCCTTCTGG; NFATc1: forward, CTCGAAAGACAGCACTGGAGCAT; reverse, CGGCTGCCTTCCGTCTCATAG; TRAP: forward, CTGGAGTGCACGA-TGCCAGCGACA; reverse, TCCGTGCTCGGCGATGGACCAGA; OSCAR: forward, TGCTGGTAACGGATCAGCTCCCCAGA; reverse, CCAAGGAGCCAGAACCTTCGAA-ACT. *Dmp1*: forward, CCAGAGGGACAGGCAAATAG; reverse, CTGGACTGTGTG-GTGTCTGC. *Mepe*: forward, AGCAAATGCCAGAGACTAAGCCC, reverse, TGAGG-CCCTCTGGCGTCATTCA. *Sost*: forward, CCACAGAGGTCATCCCA, reverse, GACACATCTTTGGCGTCATAG. *E11/gp38*: forward, ACCGTGCCAGTGTTGTTCTG, reverse, AGCACCTGTGGTTGTTATTTTGT. *Phex*: forward: GAAAGGGGACCAACC-GAGG. *FGF23*: forward, ATGCTAGGGACCTGCCTTAGA, reverse, AGCCAAGCA-ATG GGG AAGTG.

Micro-CT analysis

The long bones or vertebrae were dissected free of soft tissue from 12-week-old mice, fixed in 70% ethanol, and analyzed using a Scanco micro-CT-80 scanner (Scanco Medical, Bassersdorf, Switzerland). The samples were scanned at a voltage of 75 kVp and a resolution of 12 μm per pixel. For trabecular morphometric analysis, bone volume per tissue volume (BV/TV), trabecular thickness (Tb.Th), and trabecular separation (Tb.Sp) were performed using a native analysis system of the micro-CT to quantify 100 sections at the primary trabecular bone of the lower femoral metaphysis as areas of interests. For analysis of femoral cortex evaluation, the cortical thickness (Ct.Th) was assessed using the same system as described above, using the mid-shaft femur of 100 sections. The three-dimensional structure was constructed using 100 sections of the primary trabecular bone of metaphysis. A total of 50

sections of the mid-shaft spinal column were chosen as areas of interests to calculate the trabecular statistics of spinal column.

Western blotting

Cells and tissues were lysed with 2% SDS with 10% glycerol, 10 mM Tris-HCl (pH 6.8), 10 mM dithiothreitol, and 1 mM phenylmethylsulfonyl fluoride. Lysates were centrifuged and the supernatants were separated by SDS-PAGE and blotted onto a nitrocellulose membrane. The membrane was then probed with antibodies against the following proteins: P-S6 (Ser235/Ser236) (#4858), p-NF- κ B (Ser536) (#3033), and NF- κ B (#8242) (Cell Signaling Technology); histone H1 (sc-393358), S6 (sc-74459), and β -actin (sc-47778) (Santa Cruz Biotechnology); and p-IKK β (Ser180/Ser181) (BS4237; Bioworld, Irving, TX, USA). An ECL kit (Perkin–Elmer, San Jose, CA, USA) was used for visualization.

Enzyme-linked immunosorbent assay (ELISA)

IL-19 or G-CSF concentration was measured by ELISA (RK00163 for mouse, Abclonal; D1900 for human, R&D Systems; RK00048 for mouse, Abclonal) in the mice or human serum according to the manufacturer's instructions.

Mineralization assay

For osteogenic induction, the primary osteoblasts were first seeded in tissue-culture plates with α -MEM containing 10% FBS and cultured until the cells reached 70% confluence. To initiate the osteogenic differentiation, complete medium supplemented with β -glycerophosphate (10 mM) and L-ascorbic acid-2-phosphate (50 μ M) was added, and the differentiation medium was replaced every 2 days. Alizarin red staining was carried out according to standard techniques at day 14 (ARS, Solarbio, Beijing, China).

In vitro osteoclast culture

The bone marrow was flushed from femurs and tibiae of 12-week-old mice with α -MEM and plated on 60-mm tissue-culture plates in α -MEM containing 10% FBS and 10 ng/ml

recombinant mouse M-CSF. Cells were incubated at 37°C with 5% CO₂ overnight. Nonadherent cells were collected to Ficoll–Hypaque gradient centrifugation for purification of BMMs. For osteoclastogenesis, BMMs were incubated with osteoclast differentiation medium including 10 ng/ml recombinant M-CSF (416-ML; R&D Systems, Minneapolis, MN, USA) and 100 ng/ml recombinant RANKL (462-TEC; R&D Systems, Minneapolis, MN, USA). Mature osteoclast (multinucleated, large spread cells) began to form at day 4 after RANKL induction. The cells were then collected to qPCR to confirm their osteoclast identity.

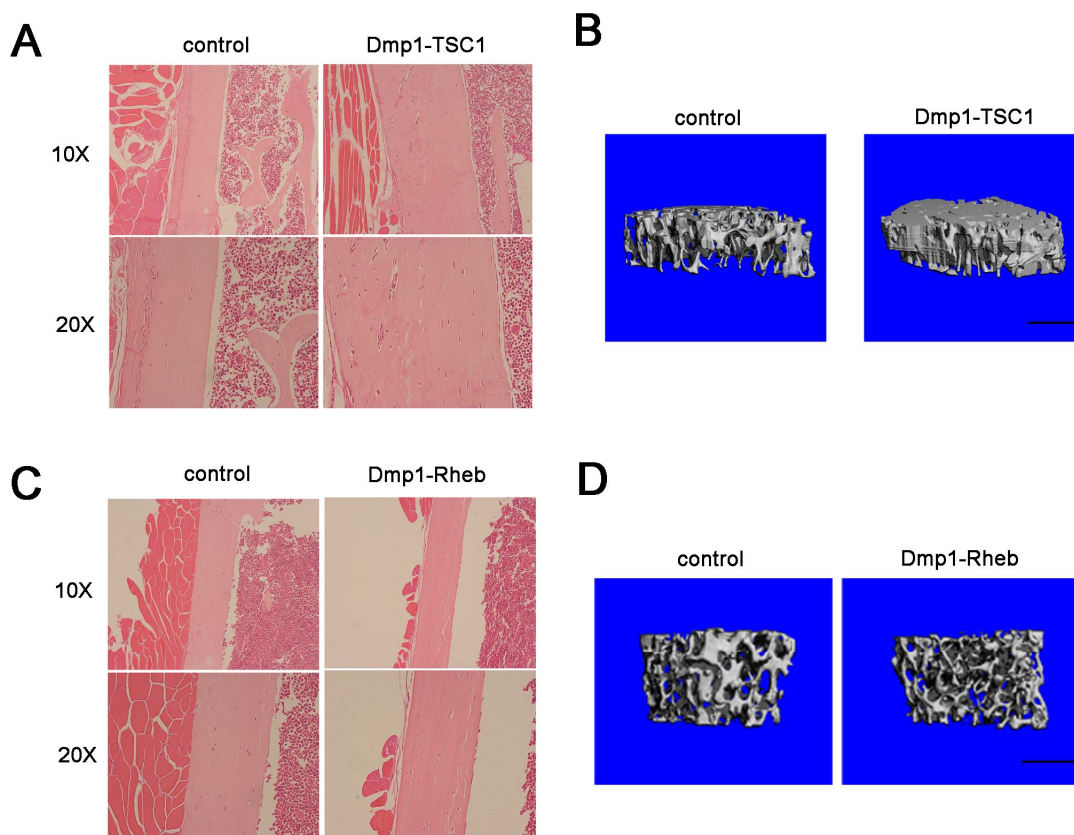


Figure S1. TSC1 loss increased and Rheb loss decreased bone formation in mice. (A) H&E staining of long bone from 12-week-old Dmp1-TSC1 and control mice. (B) Representative images of micro-CT analyses of the structure of metaphyseal trabecular bone in 12-week-old Dmp1-TSC1 and control mice. Scan bar, 1 mm. (C) H&E staining of long bone from 12-week-old Dmp1-Rheb and control mice. (D) Representative images of micro-CT analyses of the structure of metaphyseal trabecular bone in 12-week-old Dmp1-Rheb and control mice. Scale bar, 1 mm. Data are representative of three independent

experiments.

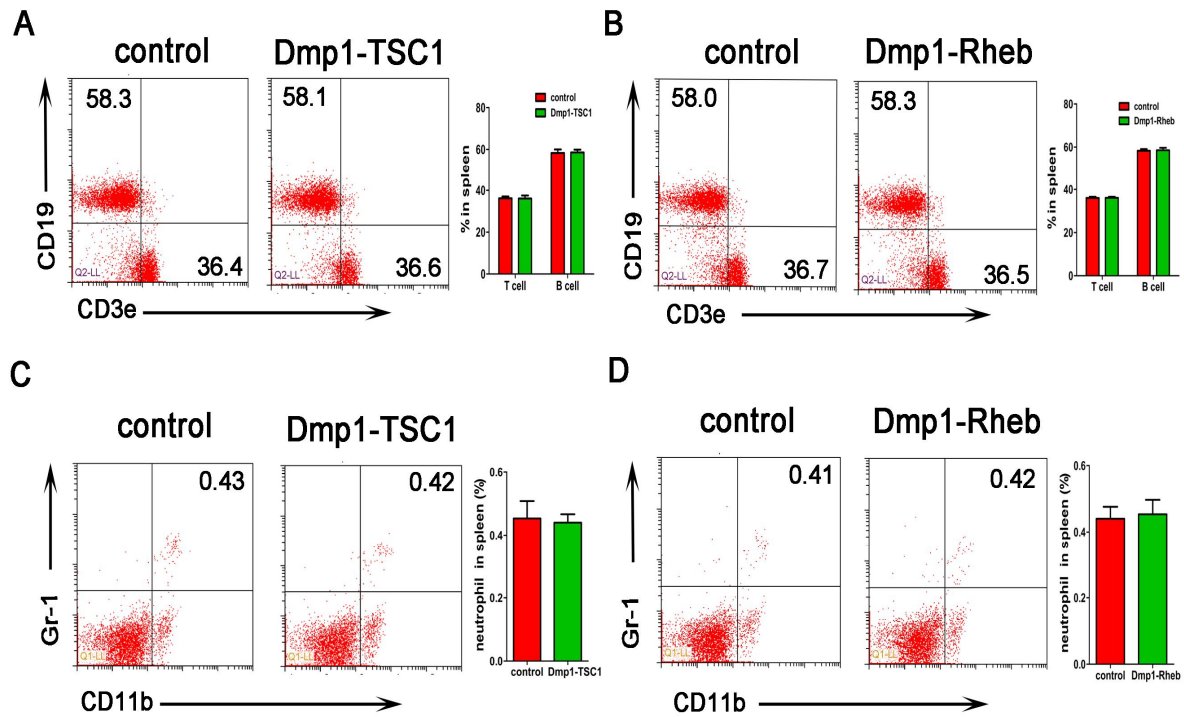


Figure S2. Osteocyte mTORC1 did not affect spleen T cell, B cell and neutrophil numbers in mice. (A) FACS analysis of T and B cells in spleen of 12-week-old Dmp1-TSC1, and control mice (mean \pm SD, n = 6). (B) FACS analysis of T and B cells in spleen of 12-week-old Dmp1-Rheb and control mice (mean \pm SD, n = 6). (C) FACS analysis of neutrophils in spleens of 12-week-old Dmp1-TSC1 and control mice (mean \pm SD, n = 6). (D) FACS analysis of neutrophils in spleens of 12-week-old Dmp1-Rheb and control mice (mean \pm SD, n = 6). Data are mean \pm SD of three independent experiments; ns, not significant; * $p < 0.05$; ** $p < 0.01$; *** $p < 0.001$.

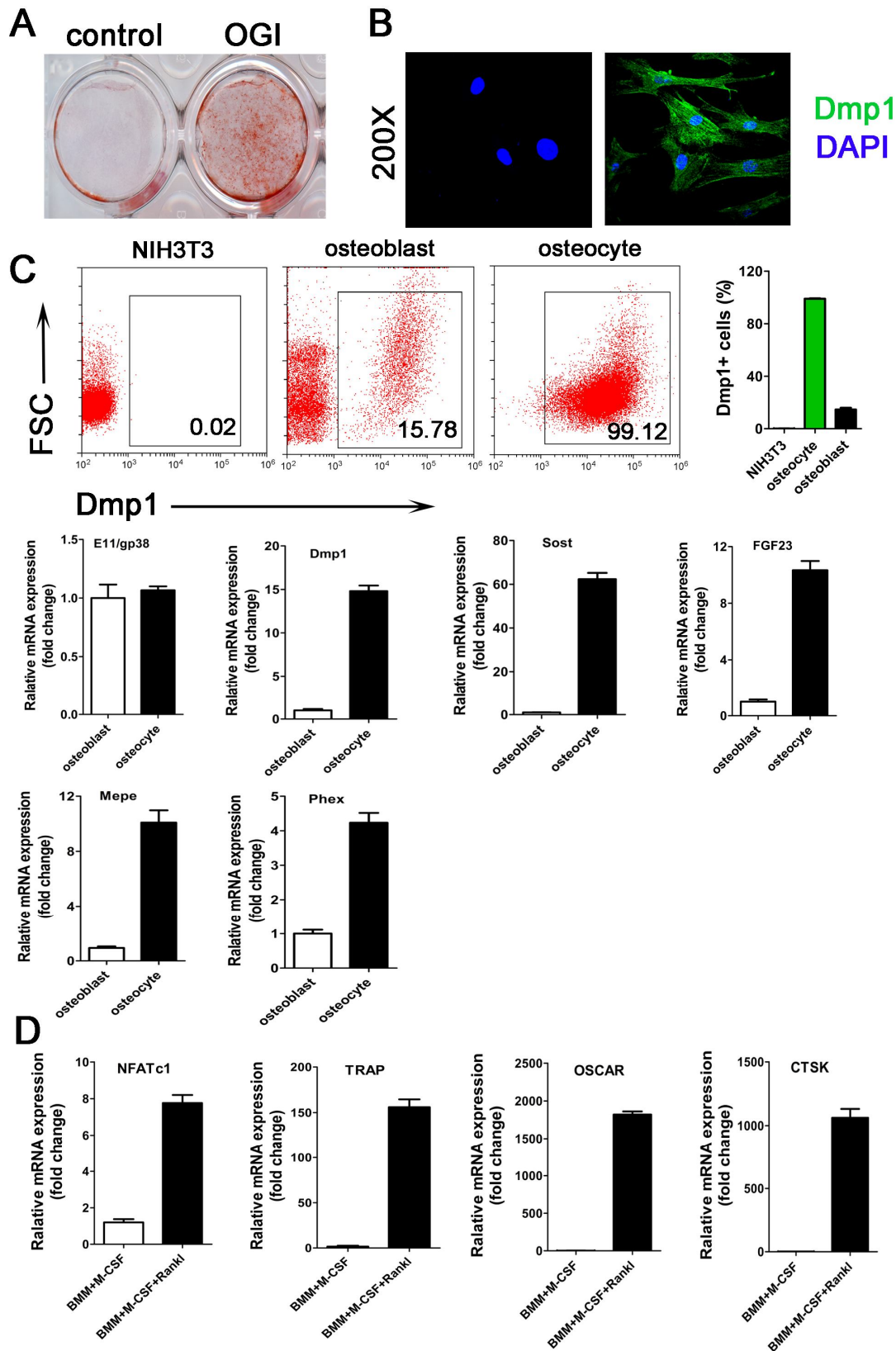


Figure S3. Identification of primary cultured osteocytes, osteoclasts and osteoblasts. (A) Alizarin red staining (AR-S) of primary osteoblastic cells on the 14th day of osteogenic induction. control: uninduced group, OGI: osteogenic induction. (B) Long bones were

aseptically dissected from skeletally mature 12-week-old mice. The bones were processed separately by serial digestion as described in Materials and Methods. After 7 days in culture, osteocytes from the bone particle outgrowth displaying an osteocyte-like morphology also stained positive for Dmp1 (green). Left, negative control, only secondary antibody added. (C) Primary osteoblasts and osteocytes were isolated from calvaria of newborn mice and long bone of 12-week-old mice respectively, FACS analysis of Dmp1⁺ cells (mean \pm SD, n = 3). NIH3T3 cells were used as a negative control. Primary osteoblasts were also used as a control. Total RNA were collected and qPCR was performed to assess the expression of the indicated genes (mean \pm SD, n = 3). (D) BMMs were cultured with M-CSF alone or M-CSF and RANKL for 4 days. Total RNA was collected and qPCR was performed to assess the expression of the indicated genes (mean \pm SD, n = 3). Data are mean \pm SD of three independent experiments; ns, not significant; * p < 0.05; ** p < 0.01; *** p < 0.001.

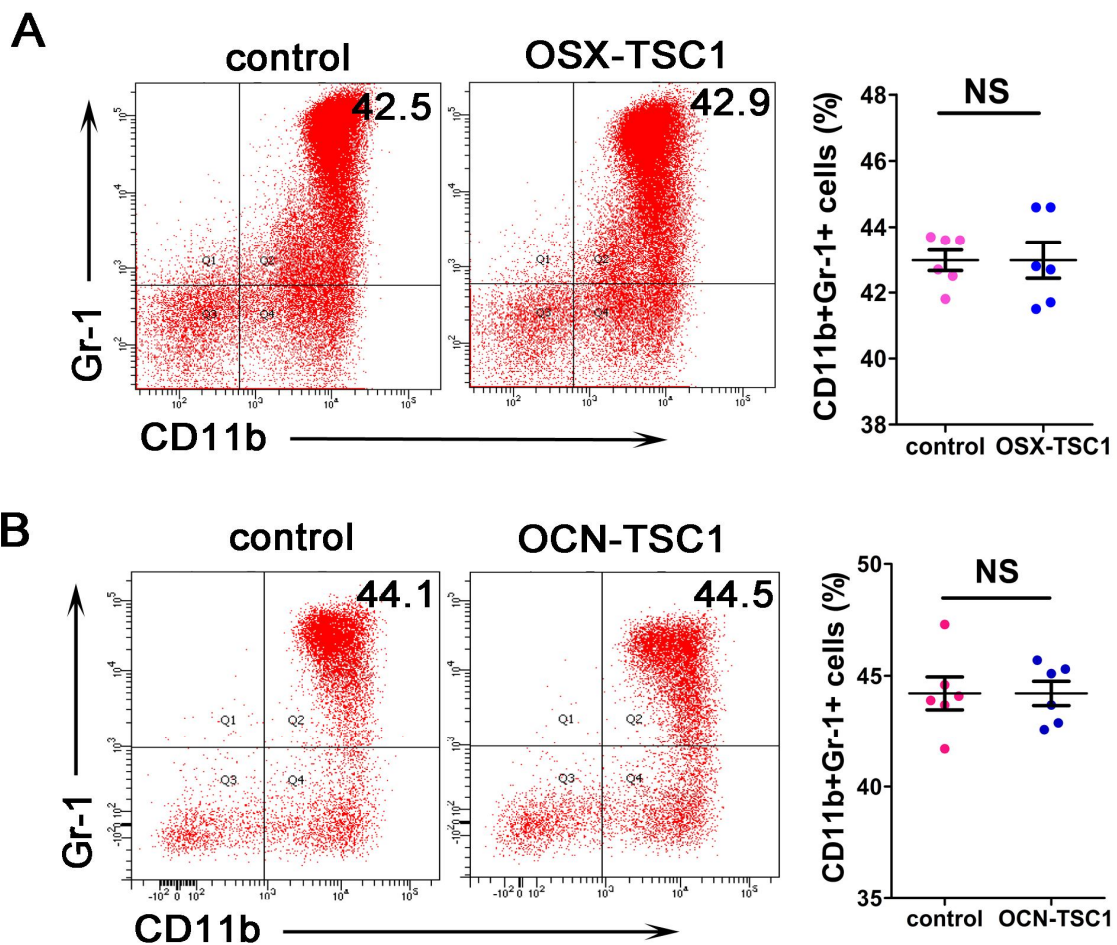


Figure S4. No significant changes in neutrophil numbers were observed between OCN-TSC1, OSX-TSC1 KO, and control mice.

(A) FACS analysis of BM CD11b⁺Gr-1⁺ neutrophils in OSX-TSC1 and control mice (mean \pm SD, n = 6). (B) FACS analysis of BM CD11b⁺Gr-1⁺ neutrophils in OCN-TSC1 and control mice (mean \pm SD, n = 6). Data are mean \pm SD of three independent experiments; ns, not significant; * p < 0.05; ** p < 0.01; *** p < 0.001.

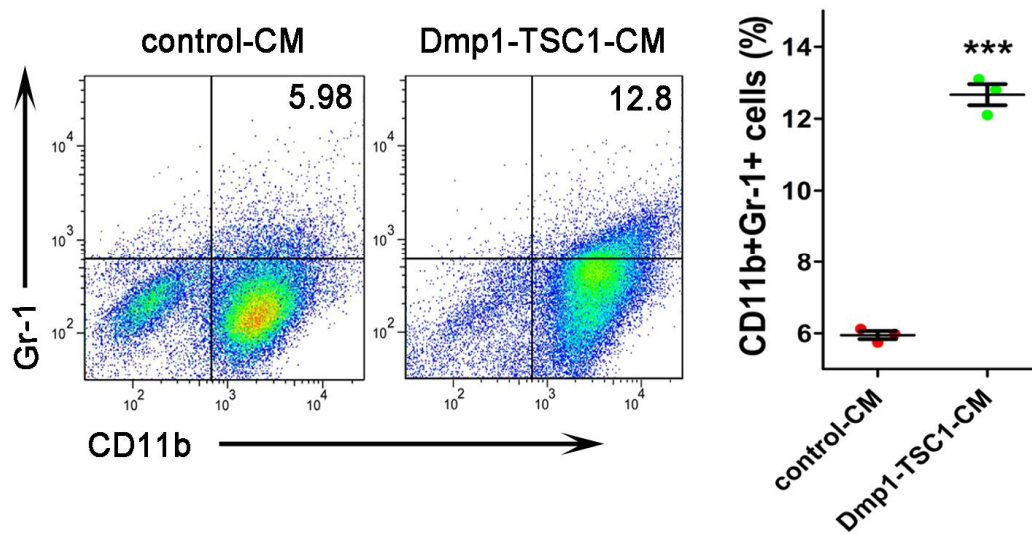


Figure S5. Osteocytes regulate granulopoiesis *in vitro*. BM cells from C57BL/6 mice were cultured in CM from osteocytes obtained from Dmp1-TSC1 and control mice for 10 days. FACS analysis of CD11b⁺Gr-1⁺ cells (mean \pm SD, n = 3). Data are mean \pm SD of three independent experiments; ns, not significant; * p < 0.05; ** p < 0.01; *** p < 0.001.

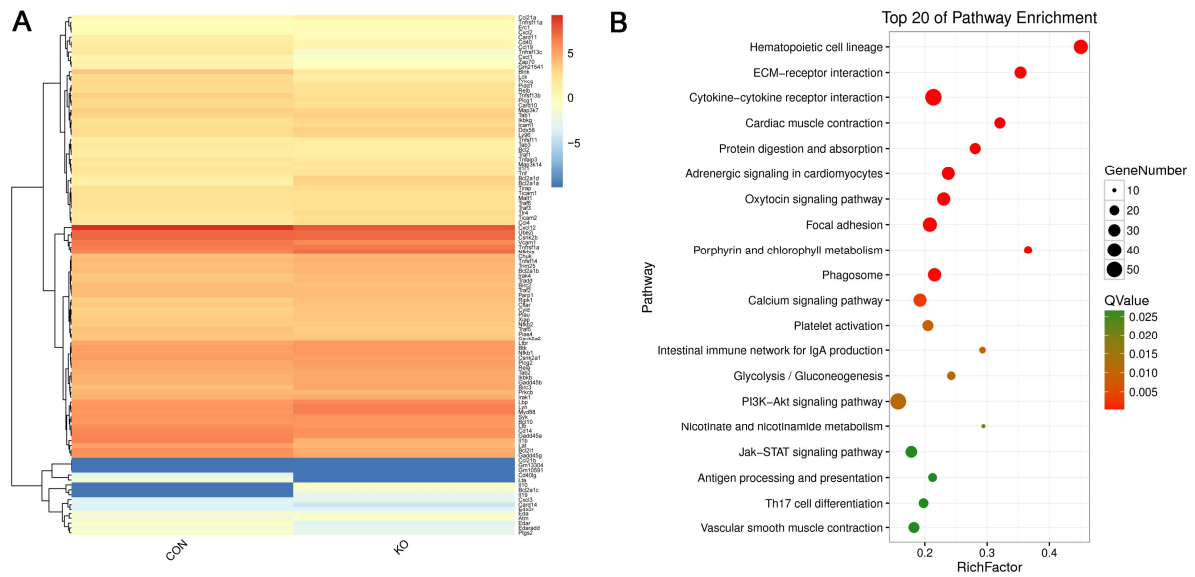


Figure S6. mRNA profiles in osteocytes from Dmp1-TSC1 and control mice. (A) The hierarchical cluster analysis of differentially expressed mRNAs in osteocytes from Dmp1-TSC1 and control mice. (B) Top 20 significantly enriched KEGG pathways of differentially expressed mRNAs. The size and color of each bubble represent the amount of differentially expressed mRNAs enriched in the pathway and enrichment significance, respectively.

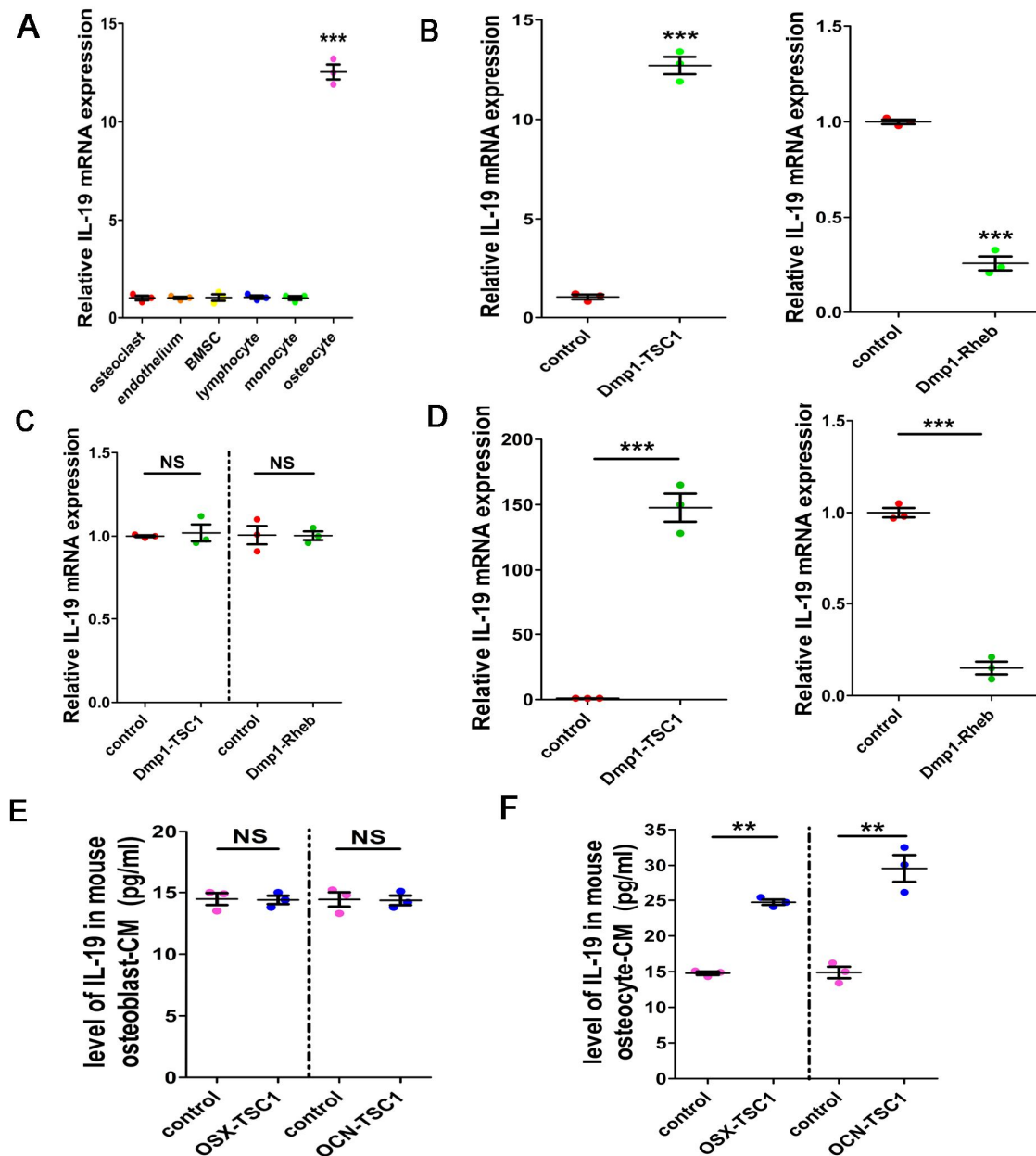


Figure S7. IL-19 is mainly secreted by osteocytes via an mTORC1-dependent mechanism. (A) The level of IL-19 mRNA in osteocytes, osteoclasts, lymphocytes, BMSCs, and endothelial cells were detected by qPCR in the BM (mean \pm SD, $n = 3$). (B) Expression levels of IL-19 mRNA in osteocytes from Dmp1-TSC1, Dmp1-Rheb, and control mice were measured by qPCR (mean \pm SD, $n = 3$). (C) The mRNA expression of IL-19 in isolated monocytes (Miltenyi, Bergisch Gladbach, Germany, 130-110-629) from BM of Dmp1-TSC1 and Dmp1-Rheb KO mice were measured by qPCR (mean \pm SD, $n = 3$). (D) Flow cytometric sorting of Dmp1⁺ cells from primary osteocytes. the level of IL-19 mRNA were detected by

qPCR in the Dmp1-TSC1 KO, Dmp1-Rheb KO, and control mice (mean \pm SD, n = 3). (E) Primary osteoblast-CM was collected to assess the level of IL-19 by ELISA in OSX-TSC1 KO and OCN-TSC1 KO mice mice (mean \pm SD, n = 3). (F) Primary osteocyte-CM was collected to assess the level of IL-19 by ELISA in OSX-TSC1 KO and OCN-TSC1 KO mice (mean \pm SD, n = 3). Data are mean \pm SD of three independent experiments; ns, not significant; * p < 0.05; ** p < 0.01; *** p < 0.001.

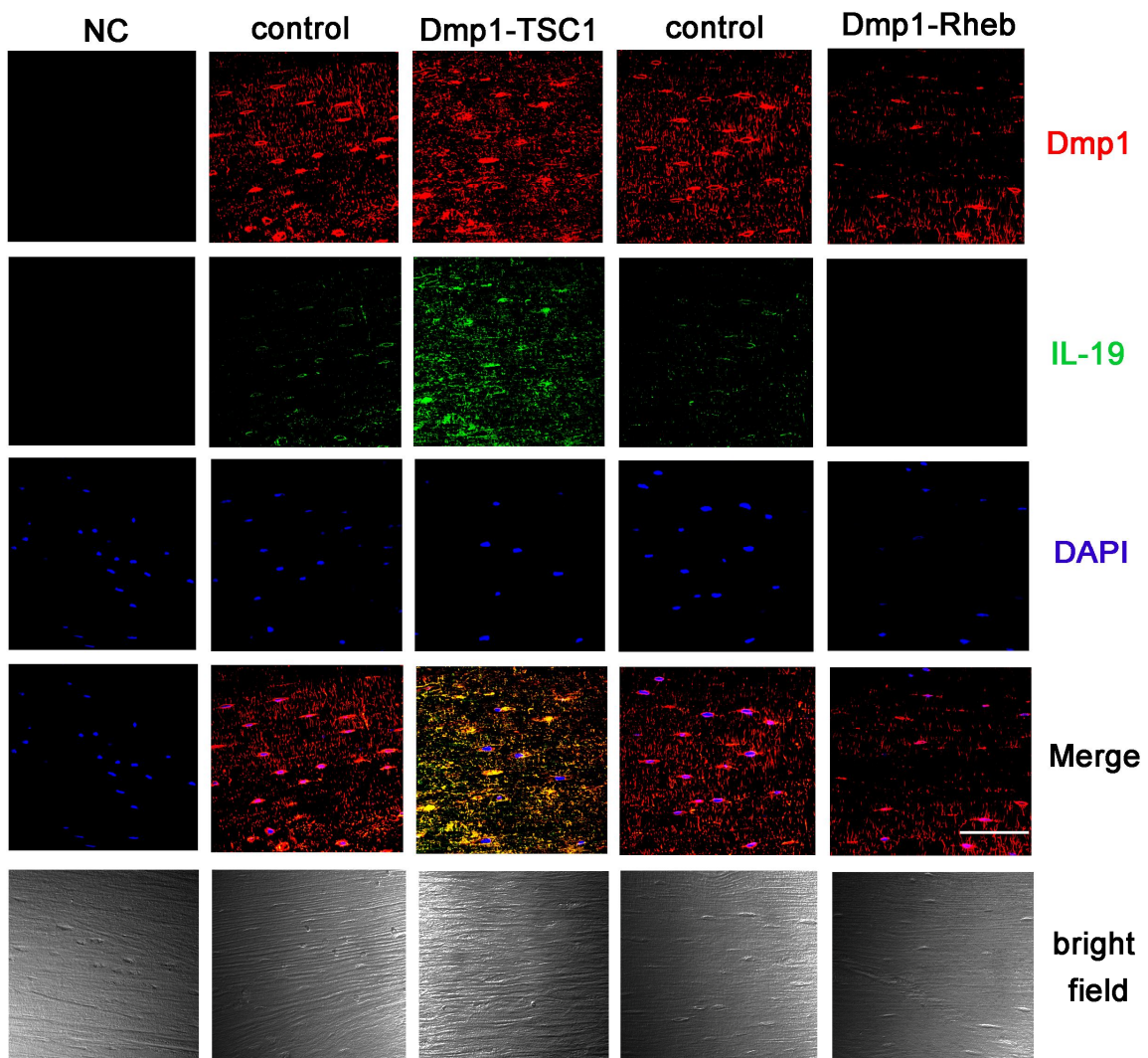


Figure S8. Expression of IL-19 in Dmp1-TSC1, Dmp1-Rheb, and control mice. Immunofluorescence microscopy of femur sections of Dmp1-TSC1, Dmp1-Rheb, and control mice. Cells were stained with anti-Dmp1 (red) and anti-IL-19 (green). Blue, nuclei visualized by DAPI stain. Scale bar, 30 μ m. NC, negative control, only secondary antibody added. Data are representative of three independent experiments.

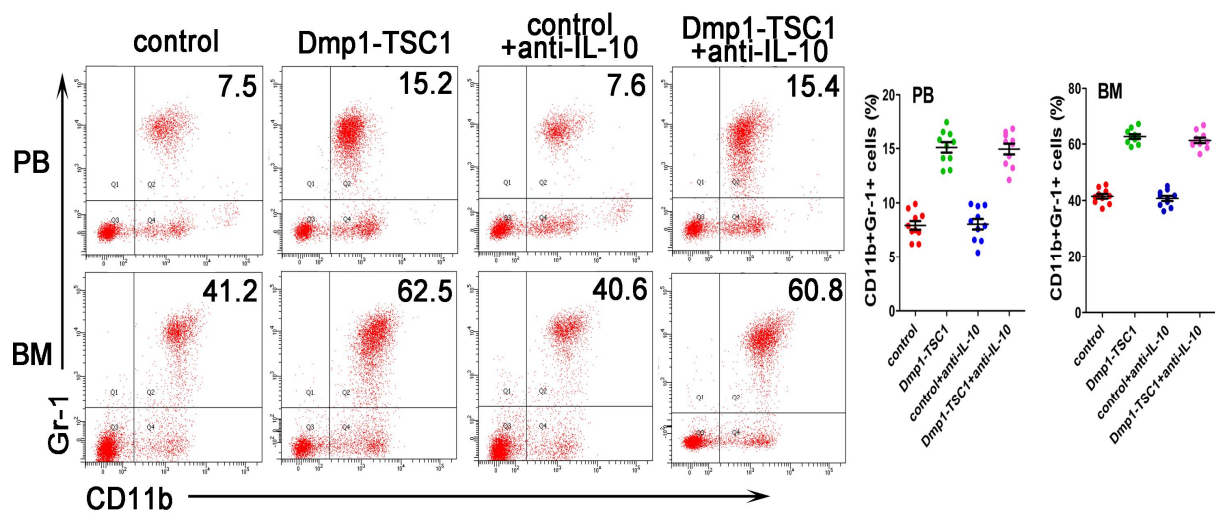


Figure S9. IL-10 did not rescue the increase of neutrophils in Dmp1-TSC1 mice.

FACS analysis of CD11b⁺Gr-1⁺ in the BM of Dmp1-TSC1 and control mice intraperitoneally injected with murine IL-10 antibody (50 μ g/kg/day) for 14 days (mean \pm SD, n = 10). (B) FACS analysis of peripheral blood CD11b⁺Gr-1⁺ neutrophils in IL-10 antibody-treated mice (mean \pm SD, n = 10). (mean \pm SD, n = 10). Data are mean \pm SD of three independent experiments; * p < 0.05; ** p < 0.01; *** p < 0.001.

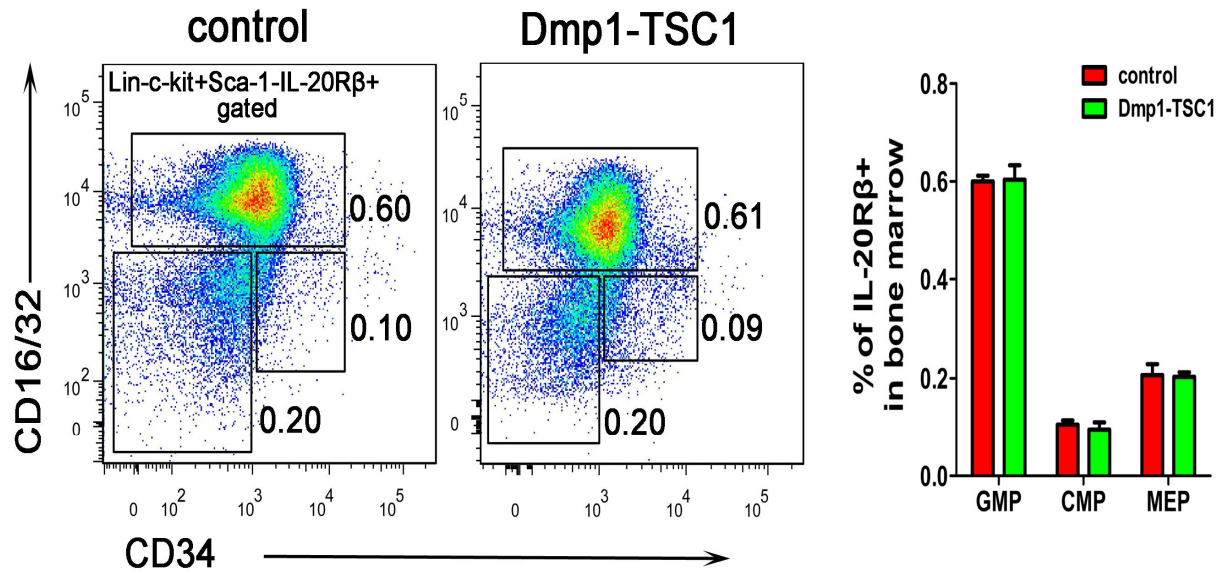


Figure S10. The IL-20R β level of GMP, MEP and CMP in Dmp1-TSC1 KO and control mice.

FACS analysis of the level of IL-20R β in GMP, CMP and MEP cells in the Dmp1-TSC1 KO and control mice (mean \pm SD, n = 6). Data are mean \pm SD of three independent experiments.

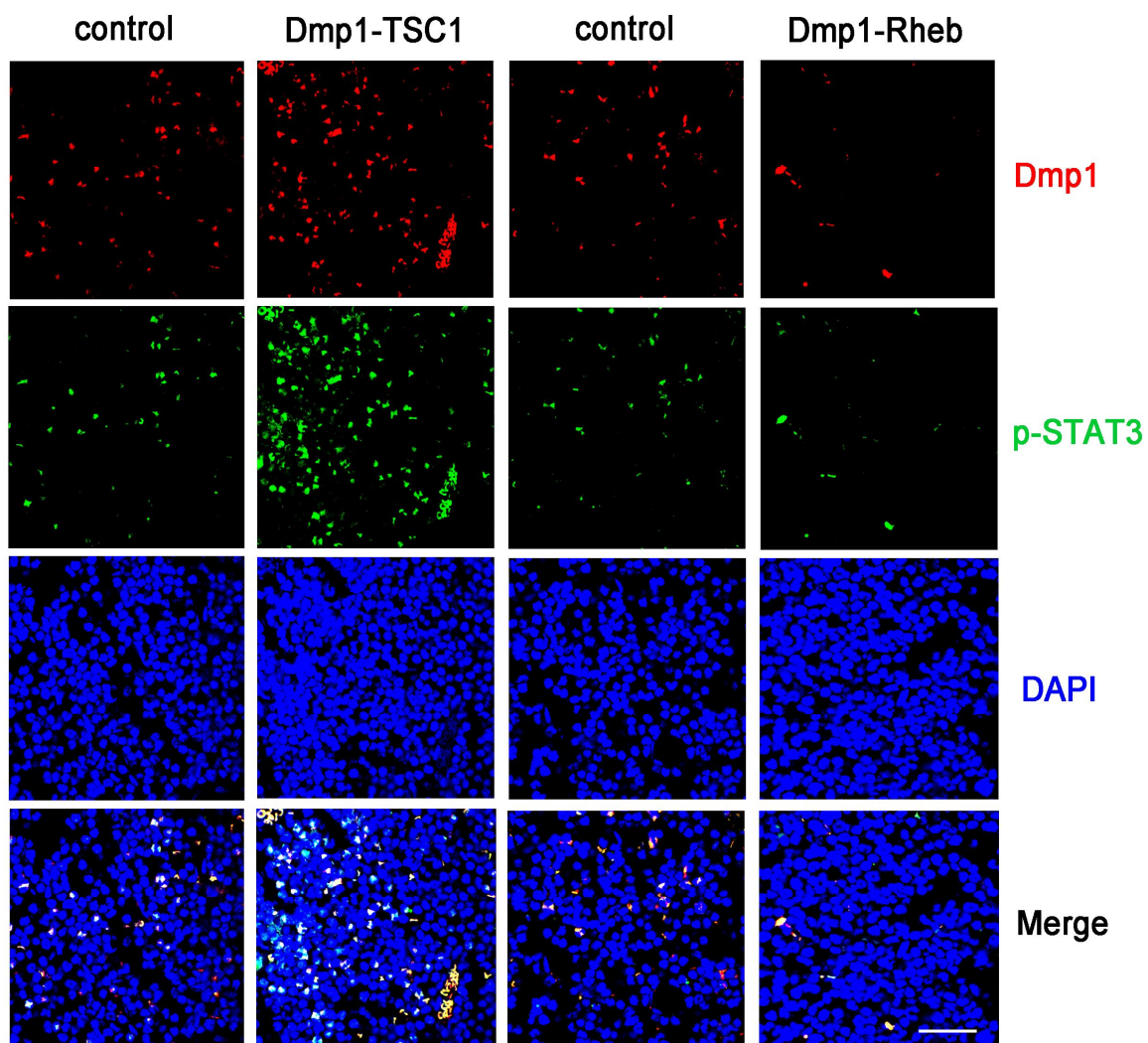


Figure S11. Phosphorylation of Stat3 in Gr-1⁺ cells of Dmp1-TSC1, Dmp1-Rheb, and control mice. Immunofluorescence microscopy of femur sections of Dmp1-TSC1, Dmp1-Rheb, and control mice. Cells were stained with anti-Gr-1 (red) and anti-p-STAT3 (green). Blue, nuclei visualized by DAPI stain. Scale bar, 30 μ m. Data are representative of three independent experiments.

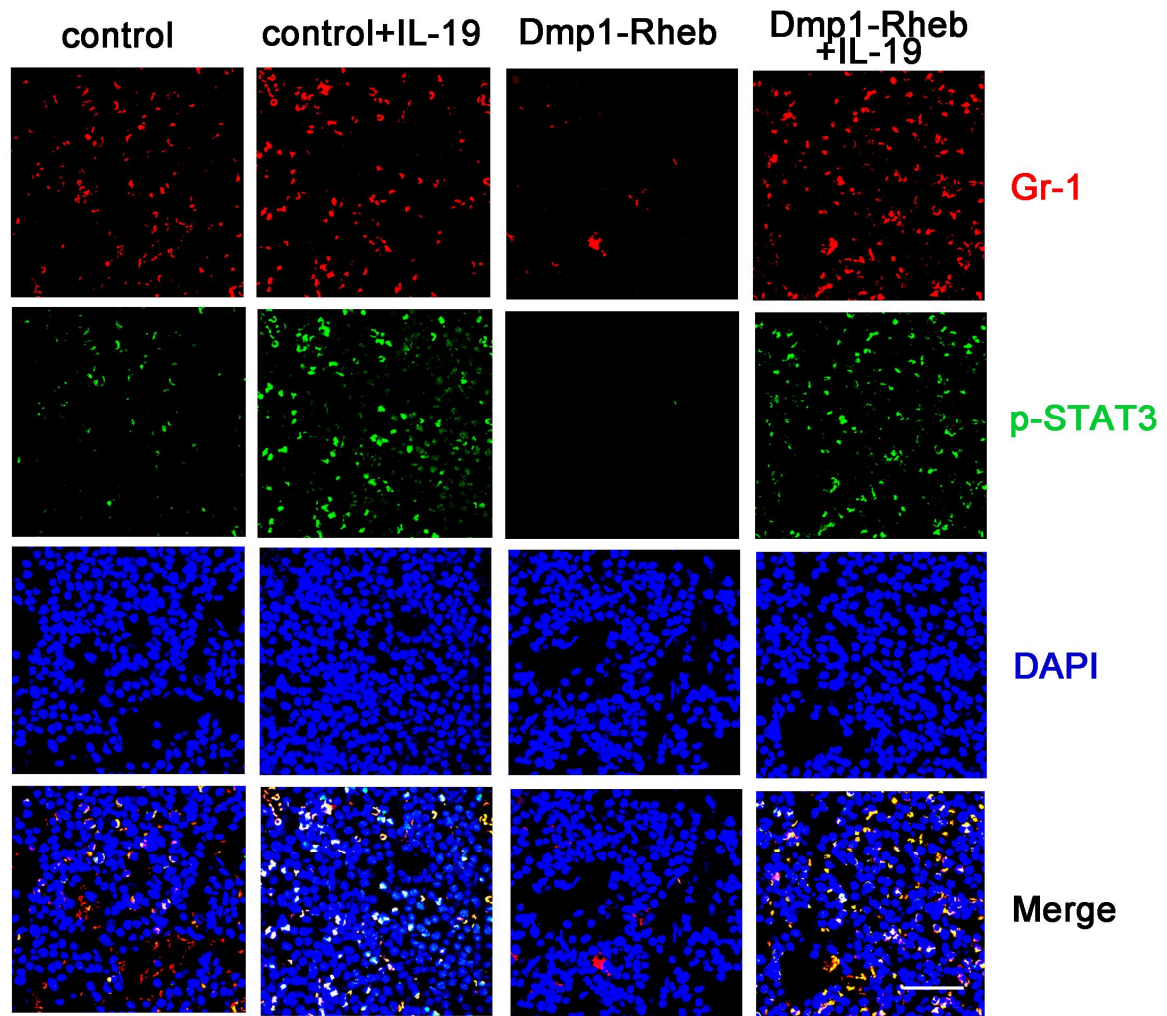


Figure S12. IL-19 stimulated Gr-1⁺ cell phosphorylation of Stat3 in Dmp1-Rheb and control mice. Immunofluorescence microscopy of femur sections of Dmp1-Rheb and control mice intraperitoneally injected with recombinant murine IL-19 (25 µg/kg/day) for 14 days. Cells were stained with anti-Gr-1 (red) and anti-p-STAT3 (green). Blue, nuclei visualized by DAPI stain. Scale bar, 30 µm. Data are representative of three independent experiments.

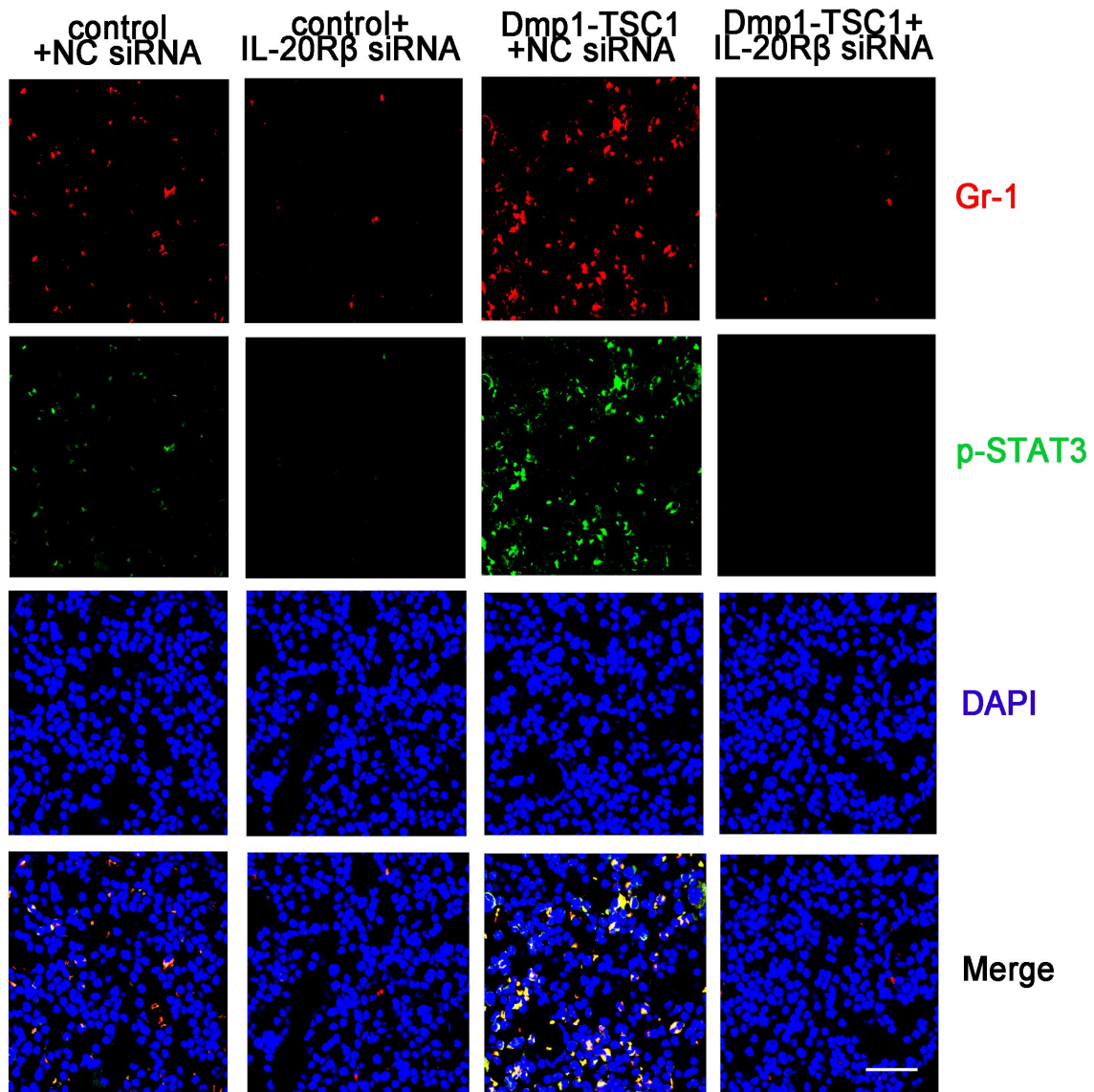


Figure S13. IL-20R β knockdown reduced p-Stat3 expression of Gr-1⁺ cells in control and Dmp1-TSC1 mice. Dmp1-TSC1 and control mice bilaterally intratibially injected into the marrow cavity with IL-20R β or NC siRNAs for 10 days. Immunofluorescence microscopy of femur sections of Dmp1-TSC1 and control mice treated with IL-20R β or NC siRNAs. Cells were stained with anti-Gr-1 (red) and anti-p-STAT3 (green). Blue, nuclei visualized by DAPI stain. Scale bar, 30 μ m. Data are representative of three independent experiments.

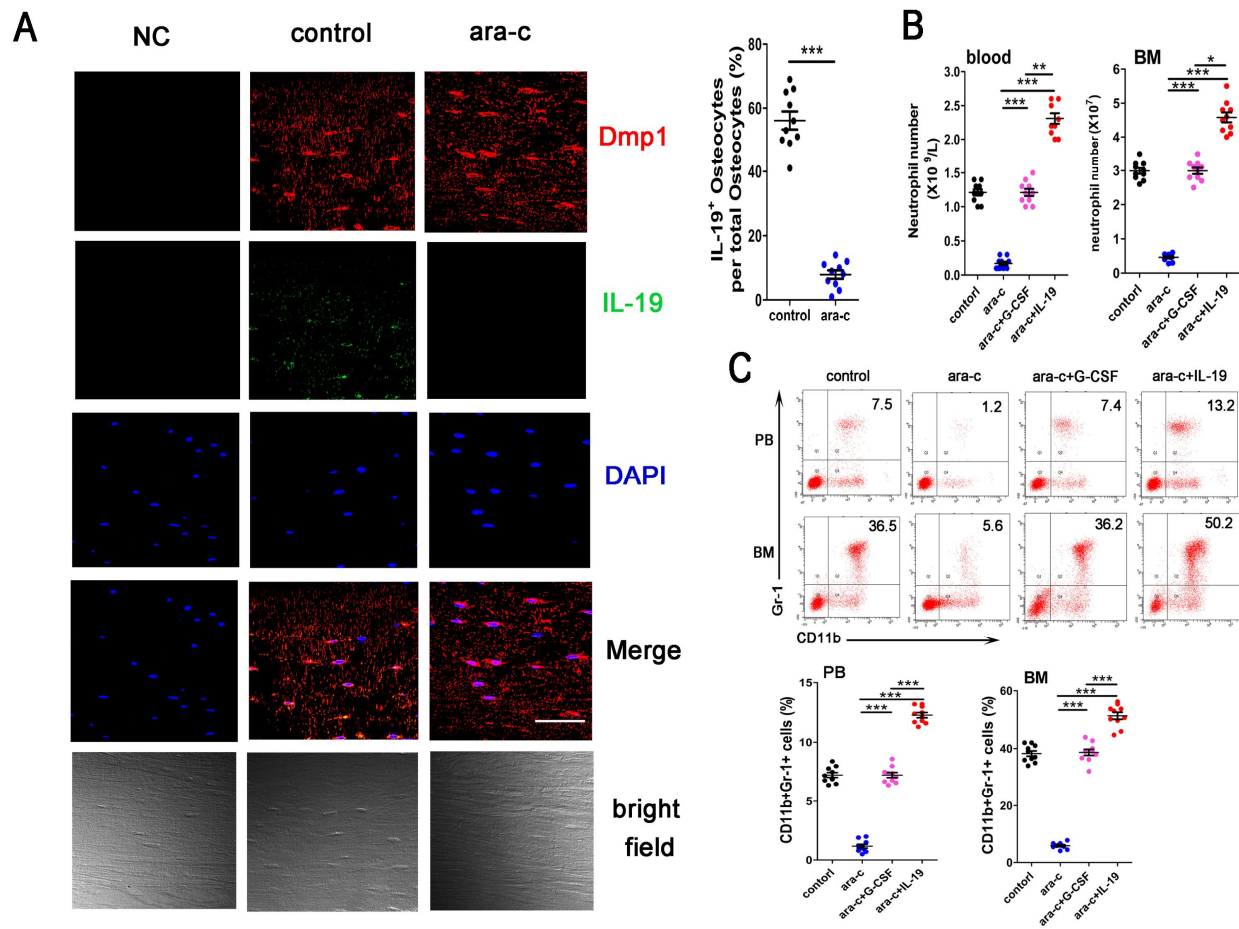


Figure S14. IL-19 prevented chemotherapy-induced neutropenia in female mice. (A) C57BL/6 female mice (2 months old) were injected with cytarabine (100 mg/kg/day) for 8 days and were sacrificed on day 9. Bone cells were stained with anti-Dmp1 (red) and anti-IL-19 (green). Blue, nuclei visualized by DAPI stain. Scale bar, 30 μ m. NC, negative control, only secondary antibody added. (B) C57BL/6 female mice (2 months old) were injected with cytarabine (100 mg/kg/day) followed by twice-daily injection of IL-19 (25 μ g/kg) or G-CSF (100 μ g/kg) from approximately 24 h after cytarabine injection; mice were sacrificed on day 9. The total number of neutrophils in peripheral blood and BM was detected (mean \pm SD, n = 10). (C) FACS analysis of BM and peripheral blood CD11b⁺Gr-1⁺ neutrophils in treated mice (mean \pm SD, n = 10). Data are mean \pm SD of three independent experiments; *p < 0.05; **p < 0.01; ***p < 0.001.

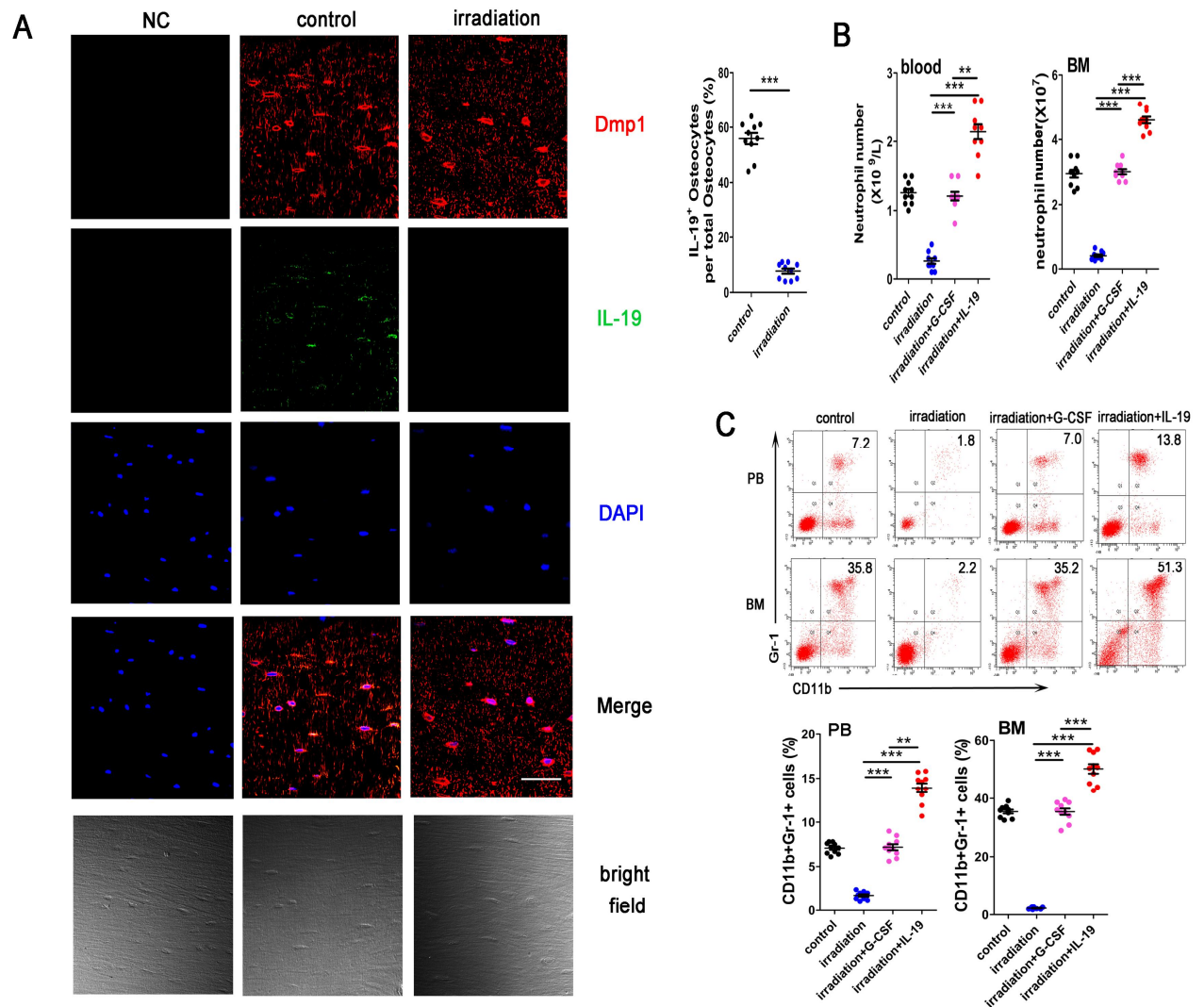


Figure S15. IL-19 prevented irradiation-induced neutropenia in female mice. (A) C57BL/6 female mice (2-months-old) received 15 exposures of 0.3 Gy/day whole-body irradiation from day 1 to day 15 to induce neutropenia. Bone cells were stained with anti-Dmp1 (red) and anti-IL-19 (green). Blue, nuclei visualized by DAPI stain. Scale bar, 30 μ m. NC, negative control, only secondary antibody added. (B) C57BL/6 female mice (2 months old) received 15 exposures of 0.3 Gy/day whole-body irradiation from day 1 to day 15 to induce neutropenia. Mice received injections of IL-19 (25 μ g/kg/day) and G-CSF (100 μ g/kg/day) from approximately 24 h after irradiation and were sacrificed on day 16. The total number of neutrophils in peripheral blood and BM was detected (mean \pm SD, n = 10). (C) FACS analysis of BM and peripheral blood CD11b⁺Gr-1⁺ neutrophils in treated mice (mean \pm SD, n = 10). Data are mean \pm SD of three independent experiments; * p < 0.05; ** p < 0.01; *** p < 0.001.

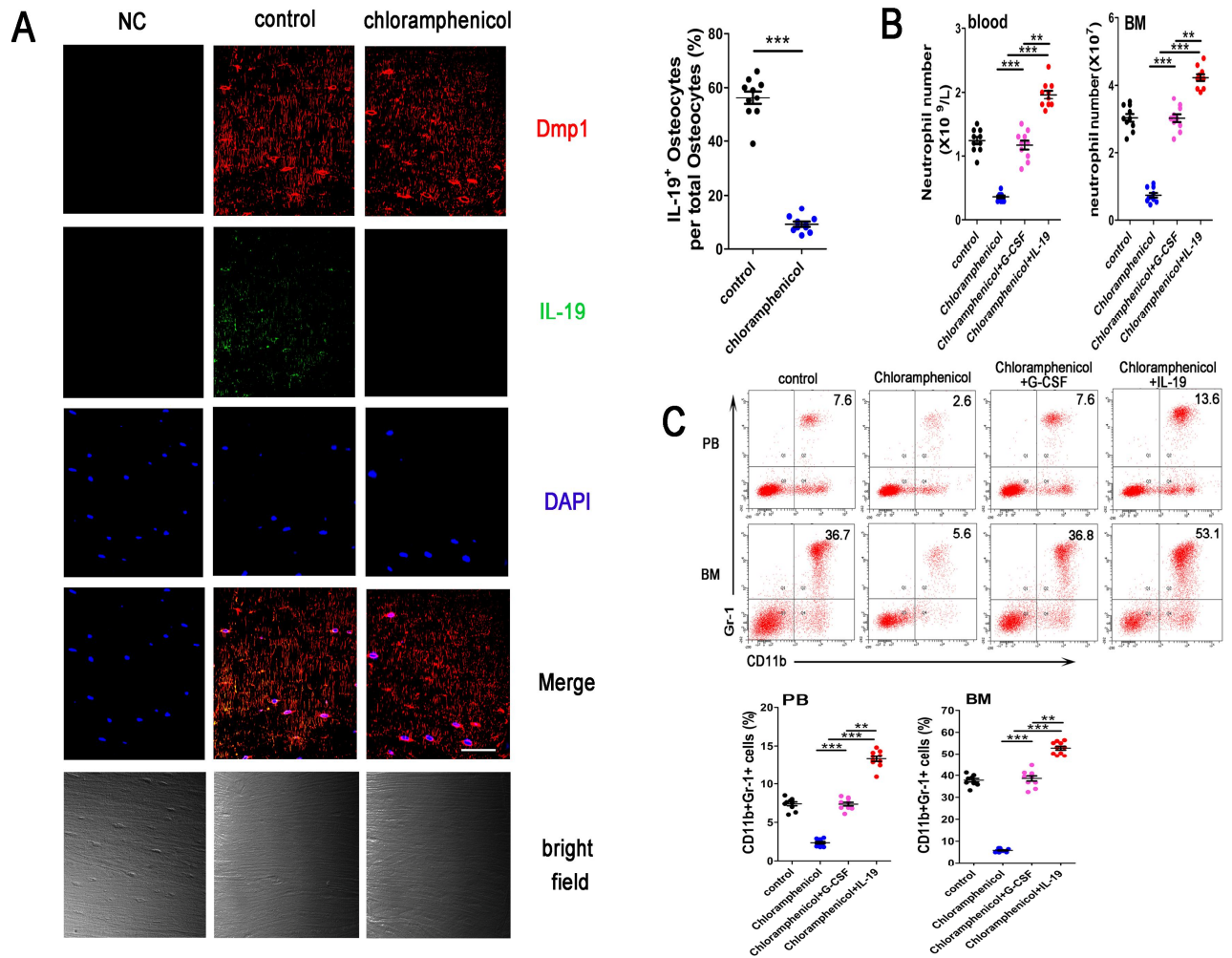


Figure S16. IL-19 prevented chloramphenicol-induced neutropenia in female mice. (A) C57BL/6 female mice (2 months old) were injected with chloramphenicol (200 mg/kg/day) for 21 days. Bone cells were stained with anti-Dmp1 (red) and anti-IL-19 (green). Blue, nuclei visualized by DAPI stain. Scale bar, 30 μ m. NC, negative control, only secondary antibody added. (B) C57BL/6 female mice (2 months old) were injected with chloramphenicol (200 mg/kg/day) followed by injection of IL-19 (25 μ g/kg/day) or G-CSF (100 μ g/kg/day) starting from 6 days after chloramphenicol injection; mice were sacrificed on day 22. The total number of neutrophils in peripheral blood and BM was detected (mean \pm SD, n = 10). (C) FACS analysis of BM and peripheral blood CD11b⁺Gr-1⁺ neutrophils in treated mice (mean \pm SD, n = 10). Data are mean \pm SD of three independent experiments; * p < 0.05; ** p < 0.01; *** p < 0.001.

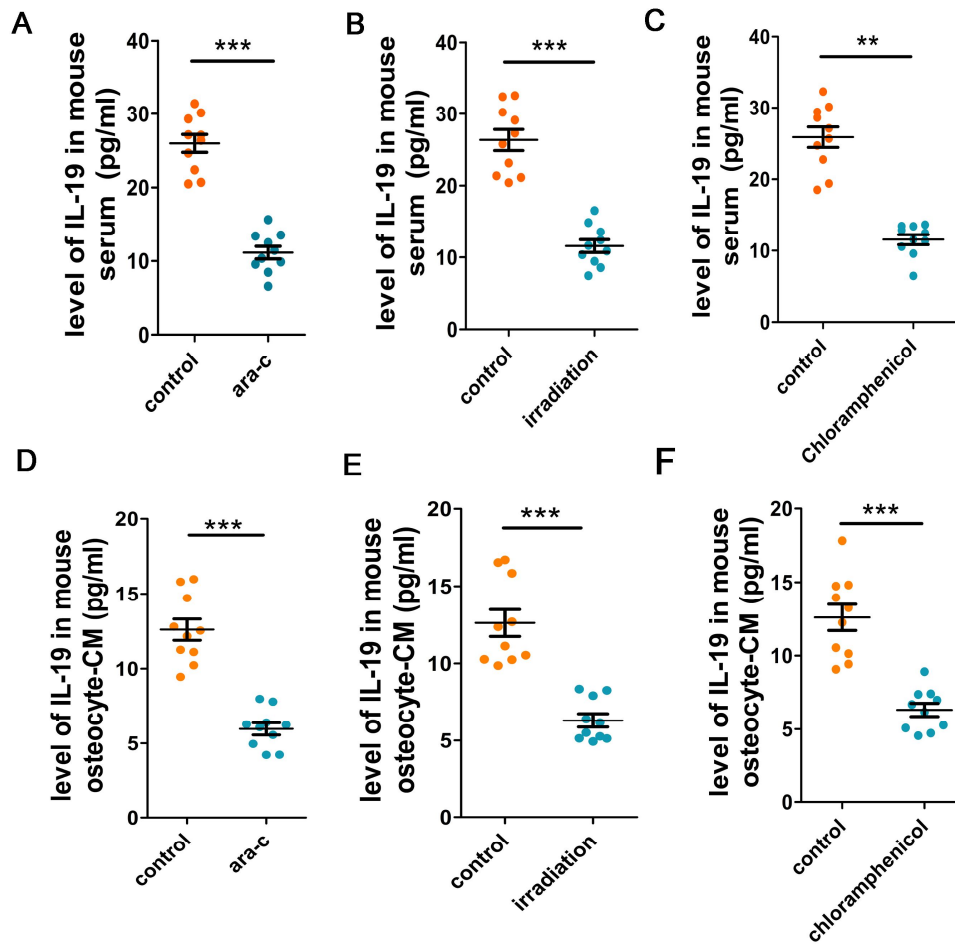


Figure S17. Cytarabine, irradiation, and chloramphenicol reduced the levels of IL-19 in serum. (A) Serum IL-19 levels in cytarabine-treated mice were detected by ELISA (mean \pm SD, n = 10). (B) Serum IL-19 levels in irradiation-treated mice were detected by ELISA (mean \pm SD, n = 10). (C) Serum IL-19 levels in chloramphenicol-treated mice were detected by ELISA (mean \pm SD, n = 10). (D) Osteocyte-CM IL-19 levels in cytarabine-treated mice were detected by ELISA (mean \pm SD, n = 10). (E) Osteocyte-CM IL-19 levels in irradiation-treated mice were detected by ELISA (mean \pm SD, n = 10). (F) Osteocyte-CM IL-19 levels in chloramphenicol-treated mice were detected by ELISA (mean \pm SD, n = 10). Data are mean \pm SD of three independent experiments; ns, not significant; * p < 0.05; ** p < 0.01; *** p < 0.001.

Table S1. Micro CT analysis of male Dmp1-TSC1 mice femur at 12 weeks of age.

parameters	control	Dmp1-TSC1	Dmp1-TSC1/control	P value
Cancellous bone				
BV/TV	0.238±0.003	0.776±0.011	3.2	0.0001
Tb.Sp [mm]	0.248±0.012	0.112±0.006	0.5	0.0008
Tb.Th [mm]	0.057±0.001	0.172±0.001	3	0.0000
Tb.N [1/mm]	4.591±0.178	4.816±0.102	1.1	0.0690
BMD [mg HA/ccm]	593.01±4.37	666.48±5.45	1.1	0.0284
Cortical bone				
Ct.Th [mm]	0.225±0.003	0.534±0.005	2.4	0.0000
outer perimeter [mm]	5.551±0.060	6.360±0.048	1.1	0.0023
inner perimeter [mm]	4.167±0.038	2.911±0.045	0.7	0.0000
BMD [mg HA/ccm]	895.11±8.17	902.38±8.05	1	0.5426

BV:bone volume

TV:total volume

Tb.N: trabecular number

Tb.Sp:trabecular separation

Tb.Th:trabecular thickness

Ct.Th:cortical bone thickness

BMD: bone mineral density

Values are shown as mean±SD (n=5).

Table S2. Routine blood examination of 12-week-old Dmp1-TSC1, Dmp1-Rheb and control littermates.

	RBC($\times 10^{12}/L$)	PLT($\times 10^9/L$)	Neutrophil($\times 10^9/L$)	Lymphocyte($\times 10^9/L$)	Monocyte($\times 10^9/L$)
control	6.54±0.12	832.23±18.72	1.5±0.48	3.6±1.12	0.2±0.06
Dmp1-Rheb	6.59±0.17	838.11±20.51	0.7±0.23	3.7±1.21	0.2±0.04
	RBC($\times 10^{12}/L$)	PLT($\times 10^9/L$)	Neutrophil($\times 10^9/L$)	Lymphocyte($\times 10^9/L$)	Monocyte($\times 10^9/L$)
control	6.65±0.15	890.33±20.13	1.5±0.50	3.5±1.06	0.2±0.06
Dmp1-TSC1	6.70±0.18	898.24±21.09	3.2±1.08	3.6±1.24	0.2±0.05

Table S3. Micro CT analysis of male Dmp1-Rheb mice femur at 12 weeks of age.

parameters	control	Dmp1-Rheb	Dmp1-Rheb/control	P value
Cancellous bone				
BV/TV	0.129±0.003	0.053±0.012	0.4	0.0002
Tb.Sp [mm]	0.381±0.011	0.219±0.010	0.6	0.0014
Tb.Th [mm]	0.027±0.011	0.030±0.014	1.1	0.0385
Tb.N [1/mm]	4.683±0.302	2.526±0.355	0.5	0.0020
BMD [mg HA/ccm]	581.52±6.32	516.73±4.72	0.9	0.0427
Cortical bone				
Ct.Th [mm]	0.078±0.002	0.082±0.005	1	0.4581
outer perimeter [mm]	3.762±0.021	3.711±0.046	1	0.4376
inner perimeter [mm]	3.026±0.017	3.121±0.022	1	0.3782
BMD [mg HA/ccm]	888.83±8.67	879.65±5.32	1	0.4219

BV:bone volume

TV:total volume

Tb.N: trabecular number

Tb.Sp:trabecular separation

Tb.Th:trabecular thickness

Ct.Th:cortical bone thickness

BMD: bone mineral density

Values are shown as mean±SD (n=5).

Table S4. Genes in Dmp1-TSC1 mouse osteocytes.

genes associated with neutrophil	Dmp1-TSC1 KO/Control
IL-19	128.000
IL-10	811.000
G-CSF	1.000
GM-CSF	1.000
Lck	0.433

Zap70	0.393
Lat	0.539
Plcg1	0.885
Prkcq	0.442
Syk	1.009
Lyn	1.514
Blnk	0.283
Btk	1.147
Plcg2	1.227
Prkecb	1.119
Card10	0.816
Card11	0.476
Card14	0.630
Bcl10	1.125
Malt1	1.176
Il1b	0.281
Il1r1	0.968
Myd88	1.893
Irak1	1.066
Irak4	1.206
Traf6	1.124
Tnf	1.062
Tnfrsf1a	1.233
Ripk1	1.445
Tradd	1.330
Traf2	1.015
Traf5	0.680
Birc2	0.950
Birc3	1.909

Eda	0.773
Edar	0.130
Edaradd	0.468
Cyld	1.366
Eda2r	0.890
Ddx58	1.424
Trim25	1.271
Lbp	1.611
Cd14	0.847
Tlr4	1.936
Ly96	1.248
Tirap	1.220
Ticam2	1.505
Ticam1	1.079
Cd40lg	0.007
Cd40	0.511
Traf3	1.120
Tnfsf11	1.165
Tnfrsf11a	1.123
Lta	0.003
Ltb	0.788
Tnfsf14	1.330
Ltbr	1.489
Map3k14	1.286
Map3k7	0.931
Tab1	1.195
Tab2	1.156
Tab3	0.685
Tnfsf13b	0.577

Tnfrsf13c	0.114
Ikbkg	1.325
Chuk	1.384
Ikbkb	1.279
Parp1	0.989
Pias4	0.899
Ube2i	1.075
Atm	2.100
Pidd1	0.645
Erc1	1.147
Nfkbia	1.631
Nfkb1	1.306
Rela	1.142
Cflar	1.299
Xiap	1.138
Bcl2l1	0.479
Bcl2	0.801
Gadd45a	0.704
Gadd45b	1.324
Gadd45g	0.613
Traf1	0.877
Bcl2a1d	4.089
Bcl2a1a	4.465
Bcl2a1b	1.168
Bcl2a1c	341.000
Nfkb2	0.983
Tnfaip3	0.736
Ptgs2	0.279
Ccl4	1.798

Cxcl1	0.364
Cxcl2	1.110
Cxcl3	1.864
Vcam1	0.667
Plau	1.288
Csnk2a1	0.963
Csnk2a2	1.008
Csnk2b	1.061
Relb	0.779
Ccl19	0.505
Gm21541	0.431
Gm13304	1.000
Gm10591	1.000
Ccl21b	1.000
Ccl21a	1.428
Cxcl12	0.358
Icam1	1.278

Table S5. Routine blood examination of 8-week-old male C57BL/6 mice treated with Cytarabine, irradiation or Chloramphenicol.

	RBC($\times 10^{12}/L$)	PLT($\times 10^9/L$)	Neutrophil($\times 10^9/L$)
control	9.19 \pm 0.12	1068.00 \pm 37.00	1.3 \pm 0.45
cytarabine	4.58 \pm 0.11	457.21 \pm 32.45	0.3 \pm 0.10
cytarabine+IL-19-1	9.23 \pm 0.16	945.24 \pm 30.24	2.6 \pm 0.75
cytarabine+IL-19-2	9.36 \pm 0.14	997.55 \pm 36.42	2.8 \pm 0.42
cytarabine+G-CSF	9.16 \pm 0.19	900.32 \pm 39.25	1.2 \pm 0.55
	RBC($\times 10^{12}/L$)	PLT($\times 10^9/L$)	Neutrophil($\times 10^9/L$)
control	9.07 \pm 0.10	1087.17 \pm 32.55	1.3 \pm 0.26
irradiation	4.12 \pm 0.12	377.16 \pm 36.41	0.2 \pm 0.12

irradiation+IL-19-1	9.02±0.07	967.34±30.15	2.4±0.36
irradiation+IL-19-2	9.07±0.08	998.59±32.47	2.6±0.11
irradiation+G-CSF	9.01±0.13	922.00±28.96	1.2±0.24
	RBC(×10¹²/L)	PLT(×10⁹/L)	Neutrophil(×10⁹/L)
control	9.26±0.35	1075.00±31.56	1.3±0.23
chloramphenicol	9.02±0.48	598.00±32.54	0.5±0.25
chloramphenicol+IL-19-1	9.24±0.41	965.00±30.18	2.2±0.52
chloramphenicol+IL-19-2	9.26±0.41	989.00±25.47	2.4±0.45
Chloramahenicol+G-CSF	9.21±0.59	920.00±26.68	1.3±0.48

Table S6. Routine blood examination of 8-week-old female C57BL/6 mice treated with Cytarabine, irradiation or Chloramphenicol.

	RBC(×10¹²/L)	PLT(×10⁹/L)	Neutrophil(×10⁹/L)
control	6.38±0.11	836.66±29.00	1.2±0.41
cytarabine	3.64±0.13	335.71±30.35	0.2±0.06
cytarabine+IL-19	6.54±0.12	791.00±25.65	2.5±0.81
cytarabine+G-CSF	6.47±0.20	780.12±22.74	1.3±0.36
	RBC(×10¹²/L)	PLT(×10⁹/L)	Neutrophil(×10⁹/L)
control	6.36±0.08	847.36±30.87	1.2±0.35
irradiation	3.08±0.06	299.92±29.61	0.3±0.14
irradiation+IL-19	6.36±0.10	784.32±25.74	2.3±0.74
irradiation+G-CSF	6.20±0.11	725.87±30.54	1.1±0.32
	RBC(×10¹²/L)	PLT(×10⁹/L)	Neutrophil(×10⁹/L)
control	6.98±0.45	875.23±20.84	1.2±0.55
chloramphenicol	6.67±0.58	587.00±21.89	0.5±0.22
chloramphenicol+IL-19	6.50±0.52	741.56±28.67	2.1±0.76
Chloramahenicol+G-CSF	6.12±0.53	700.51±24.87	1.1±0.50